HHS Public Access

Author manuscript

Nature. Author manuscript; available in PMC 2010 October 15.

Published in final edited form as:

Nature. 2010 April 15; 464(7291): 1062–1066. doi:10.1038/nature08978.

Migrastatin Analogues Target Fascin to Block Tumor Metastasis

Lin Chen[1,*], **Shengyu Yang**[1,*], **Jean Jakoncic**[2], **J. Jillian Zhang**[1], and **Xin-Yun Huang**[1]

[1] Department of Physiology, Cornell University Weill Medical College, New York, New York 10065

[2] Brookhaven National Laboratory, National Synchrotron Light Source, Upton, New York 11973

Abstract

Tumor metastasis is the primary cause of death of cancer patients. Development of new therapeutics preventing tumor metastasis is urgently needed. Migrastatin is a natural product secreted by Streptomyces [1],[2], and synthesized migrastatin analogues are potent inhibitors of metastatic tumor cell migration, invasion and tumor metastasis [3–6]. Here we show that these migrastatin analogues target the actin-bundling protein fascin to inhibit its activity. X-ray crystal structural studies reveal that migrastatin analogues bind to one of the actin-binding sites on fascin. Our data demonstrate that actin cytoskeletal proteins, such as fascin, can be explored as new molecular targets for cancer treatment, similar to the microtubule protein tubulin.

To understand the molecular basis by which migrastatin analogues inhibit tumor cell migration and tumor metastasis, we pursued the biochemical identification of the protein target for macroketone. We took an affinity protein purification approach using synthesized biotin-labeled macroketone [4] (Fig. 1a). Biotin-conjugated macroketone inhibited 4T1 breast tumor cell migration with a similar potency (IC_{50} ~ 300 nM) as the non-biotinylated macroketone (IC_{50} ~100 nM) 4. 4T1 tumor cell extracts were incubated with biotin-conjugated macroketone or with free biotin. Strepavidin conjugated agarose beads were added. After extensive washes, bound proteins were eluted and resolved by SDS-PAGE. A protein of approximately 58 kDa was specifically detected in the sample from affinity-purified proteins with biotin-conjugated macroketone, but not in the sample with free biotin (Fig. 1b). This ~58 kDa protein was identified by mass spectrometry and by peptide sequence as mouse fascin 1. Fascin is the primary actin cross-linker in filopodia and is required to maximally cross-link the actin filaments into straight, compact, and rigid bundles [7–12]. Elevated expressions of fascin mRNA and protein in cancer cells have been correlated with aggressive clinical course, poor prognosis and shorter survival [13–21].

X.-Y. H: To whom correspondence should be addressed, Tel: (212) 746-6362, FAX: (212) 746-8690, xyhuang@med.cornell.edu.
*These authors contributed equally to this work.

SUPPLEMENTARY INFORMATION is linked to the online version of the paper at www.nature.com/nature.

AUTHOR CONTRIBUTIONS: L.C., S.Y., J.J.Z. and X.Y.H. conceived the project. L.C. and S.Y. performed the experiments. S.Y. and J.J. determined the structures. L.C., S.Y., J.J.Z. and X.Y.H. analyzed the data and wrote the paper.

AUTHOR INFORMATION: The coordinates and structure factors of crystal structures of fascin and of the complex of fascin and macroketone have been deposited in the Protein Data Bank under accession numbers 3LLP and 3LNA. Reprints and permissions information is available at www.nature.com/reprints. The authors declare no competing financial interests.

Next we verified that macroketone indeed directly interacts with fascin. We purified recombinant GST-tagged fascin to homogeneity from *Escherichia coli* (Supplementary Fig. 1a). Purified fascin, but not GST control, specifically interacted with biotin-conjugated macroketone (Fig. 1c). Moreover, an excess amount of non-biotinylated macroketone efficiently competed the binding between fascin and biotin-conjugated macroketone (Supplementary Fig. 1b). Another migrastatin analogue, macrolactam, also competed with biotin-conjugated macroketone for binding to fascin. Collectively, these data demonstrate that fascin is a protein target of macroketone.

We then examined the biochemical effect of macroketone on the activity of fascin. We have used three different approaches to investigate the effect. First, we used purified recombinant fascin protein, and investigated its actin-bundling activity by the F-actin pelleting assay [9]. In this low-speed centrifugation assay, the pellets contain bundles of F-actin polymers [9]. Purified fascin increased the amounts of F-actin bundles in the pellets (Fig. 1d, e). While macroketone alone had no effect on the formation of F-actin bundles, macroketone significantly decreased the fascin-induced bundling of F-actin polymers (Fig. 1d, e). Second, we used the fluorescence microscopy to visualize the fascin-regulated F-actin filament bundles in the absence and presence of macroketone (Supplementary Fig. 2a, b). Addition of fascin induced the formation of F-actin bundles, as revealed by the staining of F-actin filaments with Rhodamine-conjugated phalloidin (Supplementary Fig. 2a). In contrast, in the presence of macroketone, formation of F-actin bundles was largely (>80%) inhibited (Supplementary Fig. 2a, b). Third, electron microscopy was used to examine the actin bundles (Fig. 1f and Supplementary Fig. 2c). The EM examination revealed that macroketone decreased the thickness of the bundles. These data demonstrate that macroketone inhibits the actin-bundling activity of fascin.

To reveal the structural basis for the inhibition of fascin function by migrastatin analogues, we have solved the X-ray crystal structures of fascin without and with a migrastatin analogue (Fig. 2). We determined the native fascin structure and the structure of fascin-macroketone complex at 1.8 Å and 2.7 Å, respectively (Fig. 2 and Supplementary Table 1). The overall structure of fascin exhibits four β-trefoil folds, with each β-trefoil comprising of six two-stranded β-hairpins (Fig. 2a–c, Supplementary Fig. 3–5, and Supplementary Table 2–4). This structure is similar to one fascin structure deposited in the protein structural dada base (Supplementary Fig. 6). The overall domain arrangement of fascin-macroketone complex is very similar to that of the native fascin (Fig. 2d). The bound macroketone molecule sits at the surface of trefoil 4, on the side facing the cleft between trefoil 4 and trefoil 1 (Fig. 2d, e and Supplementary Fig. 7). Macroketone is held in place by interacting with the side chains of His392, Glu391, Ala488, Lys471, and His474 as well as the alpha carbon of Asp473 (Fig. 2d, e and Supplementary Fig. 8). His392 and His474 contribute to the binding of macroketone through hydrogen bonds (Fig. 2e). The interaction between fascin and macroketone is further stabilized by the *van der Waal*s force between the macrolide ring carbon and residue Glu391, Ala488, Lys471 and Asp473 (Fig. 2e). These structural data are consistent with our previous structure-activity studies on migrastatin analogues that the macrolide ring, instead of the long side-chain of migrastatin, was important for the inhibitory function on tumor cell migration[4].

The structure of the fascin-macroketone complex immediately suggests a possible biochemical mechanism by which macroketone inhibits the actin bundling activity of fascin. The macroketone binding site is one of the actin-binding sites on fascin (Fig. 3a). Therefore, we propose that macroketone binding interferes with the binding of actin filament to fascin. Fascin functions as a monomer to bundle actin filaments, and it has been proposed that fascin has two actin-binding sites for this bundling activity [22]. Previous mutagenesis studies implied that both the N- and the C -termini of fascin contribute to actin binding. Our crystal structure implicates that the N- and C-termini constitute one of the actin-binding sites (Fig. 3a). Both the N-and C-termini are located in the same cleft (Fig. 3a). Furthermore, a stretch of residues from 29 to 42 at the N-terminal, which has similarity to an actin-binding site of MARCKS (myristoylated alanine-rich C-kinase substrate) [23], is also facing the trefoil 1–4 cleft (Fig. 3a). Moreover, the actin bundling activity of fascin is negatively regulated by a protein kinase C phosphorylation site (Ser39) within the N-terminal region [22] (Fig. 3a). Together, these data suggest that this cleft represents one of the actin-binding sites.

To investigate this hypothesis that macroketone binding site overlaps with one of the actin-binding sites, we mutated five residues involved in macroketone binding and examined the actin bundling activity of those fascin mutants (Fig. 3b–d). Indeed, mutations of His392, Lys471 and Ala488 decreased the actin bundling activity of fascin (Fig. 3c, d). These data demonstrate that residues involved in macroketone binding are involved in actin bundling. Furthermore, we examined the sensitivity of the actin bundling activity of Glu391 and His474 to macroketone (mutants His392, Lys471 and Ala488 were not tested due to their defective actin bundling activity). As shown in Fig. 3e and f, mutation of His474 to Ala rendered fascin resistant to macroketone treatment. Moreover, this His474 to Ala mutant fascin did not bind to biotin-macroketone (Fig. 3g). Taken together, our data demonstrate that several fascin residues (such as His392, Lys471 and Ala488) involved in macroketone binding also contribute to actin binding. Hence, the macroketone binding site is one of the actin-binding sites.

To further critically evaluate that macroketone inhibits fascin to decrease tumor cell migration, invasion and metastasis, it would be the best to have a fascin mutant that does not bind to macroketone, but retains its actin-bundling activity. This mutant fascin should confer resistance to macroketone in tumor cell migration, invasion and metastasis. Our above data showed that His474 is essential for the macroketone binding, but not for actin-bundling (Fig. 3). To confirm that fascin His474Ala mutant could support tumor cell migration, invasion and metastasis, we used RNA interference to down-regulate fascin protein levels in 4T1 mouse mammary tumor cells. While two fascin shRNAs (small hairpin RNAs) knocked down the fascin protein levels, a control shRNA did not (Supplemental Fig. 9a). Fascin shRNA-treated cells grew at comparable rates as control shRNA-treated cells and non-transfected 4T1 cells in full growth medium (Supplementary Fig. 9b), suggesting fascin is not required for breast tumor cell proliferation *in vitro*. This is consistent with our previous observation that migrastatin analogues had no effect on tumor cell proliferation and primary tumor growth in mouse models [5]. Boyden chamber cell migration assay showed that fascin shRNA treatments, but not treatment with the control shRNA, decreased the serum-induced migration of 4T1 cells (Supplementary Fig. 9c). Moreover, this inhibitory effect of fascin

shRNA could be rescued by transfection of human fascin cDNA (there are two nucleotide changes without amino acid changes in this specific region) (Fig. 4a). This rescued migration was sensitive to macroketone (Fig. 4a). Although mutations of His474 to either Lys (Drosophila fascin has a Lys in the corresponding position) or Ala in human fascin also rescued the migration of 4T1 cells treated with fascin siRNAs (Fig. 4a), these rescued migrations were not inhibited by macroketone (Fig. 4a and Supplementary Fig. 9d). Additionally, we performed the rescue experiments of fascin-shRNA-treated 4T1 cells with villin, another actin-bundling protein. From Drosophila genetic studies, villin partially rescued the phenotypes of fascin mutations during *Drosophila* oogenesis [24]. Villin did not bind macroketone in vitro, and over-expression of villin in fascin-shRNA treated 4T1 cells partially rescued the migration which was insensitive to macroketone (Supplementary Fig. 9e). Similarly, expression of human wild-type fascin and His474Ala fascin mutant in fascin shRNA-treated mouse 4T1 cells rescued tumor cell invasion (Fig. 4b). The rescued invasion by wild-type fascin, but not by His474Ala mutant fascin, was sensitive to macroketone (Fig. 4b and Supplementary Fig. 9f). Moreover, fascin His474Ala mutation confers macroketone resistance in tumor metastasis (Fig. 4c, d). Fascin shRNA treatment abolished 4T1 tumor cell metastasis in mouse models (Fig. 4c,d). Macroketone significantly inhibited the metastasis in mice injected with control shRNA-treated cells. Wild-type human fascin-rescued 4T1 cells metastasized to the lung, and this metastasis was inhibited by macroketone (Fig. 4d). On the other hand, although re-expression of His474Ala mutant fascin rescued the tumor metastasis, this metastasis was insensitivity to macroketone (Fig. 4d). These results further confirm that fascin is the protein target for macroketone in its inhibition of tumor cell migration, invasion and metastasis.

With the future clinical application in mind to use fascin inhibitors for human cancer treatments, we further investigated the inhibition of lung colonization of human breast tumor cells in immune-deficient mouse models by fascin inhibitors such as fascin shRNAs and macroketone. MDA-MB-231 cells were retrovirally infected with a triple-fusion protein reporter construct encoding herpes simplex virus thymidine kinase 1, green fluorescent protein (GFP) and firefly luciferase (TGL) [25,26]. These cells were injected into the tail vein of immuno-deficient mice [NOD-SCID mice]. The lung colonization of tumor cells was monitored by non-invasive bioluminescence imaging (Fig. 4e,f, Supplementary Fig. 10a–d) [20]. A substantial attenuation of bioluminescence signal was observed within the first few days, indicating that cells that failed to metastasize were not able to survive (Fig. 4e, f). Progressively increasing signals after two weeks in mice with control shRNA-treated tumor cells indicated that cells had succeeded in metastasizing and proliferating (Fig. 4e, f). Strikingly, the presence of fascin shRNA treated cells in the lung was much less than control shRNA-treated cells (Fig. 4e, f). Therefore, fascin shRNA treatments significantly inhibited the lung colonization. Second we have further demonstrated here that macroketone could effectively block the lung colonization of human breast tumors in an animal model. As shown in Fig. 4g, macroketone reduced the lung colonization of MDA-MB-231 cells by >80%. Together, our data demonstrate the feasibility of using the inhibitors of fascin (such as macroketone and the siRNAs) as therapeutic agents for treating metastatic breast tumors.

Fascin mRNA transcript and protein levels are significantly elevated in clinically aggressive tumors [17,27]. Overexpression of fascin leads to increases in cell migration and invasion [28,29]. We have analyzed a microarray gene expression data set with 137 breast cancer samples and 16 normal breast samples from patients treated at the Memorial Sloan-Kettering Cancer Center. Breast tumor samples showed elevated fascin expressions comparing to normal samples. Moreover, we observed a significant high level of fascin transcripts in the estrogen receptor (ER)-negative group of patients (Supplementary Fig. 11a) and progesterone receptor (PR)-negative group of patients (Supplementary Fig. 11b). Immunohistology staining with anti-fascin antibody confirmed that fascin protein was up regulated in ER-negative tumors (Supplementary Fig. 11c), while ER-positive tumor cells were negative for fascin staining (note that endothelia of vessels are fascin positive). Furthermore, we analyzed fascin mRNA expression levels in the Rosetta microarray data set of 295 breast cancer patients [30]. Similarly, we found that the levels of fascin transcripts were significantly higher in ER-negative and PR-negative tumors (Supplementary Fig. 11d,e).

Overexpression of fascin contributes to a more aggressive clinical course of cancer [16]. The Rosetta data set contains detailed clinical follow-up information of breast cancer patients. Thus, we evaluated the clinical and pathological associations of fascin expression in breast cancer patients. Kaplan-Meier analyses showed that higher fascin expression was associated with lower overall survival (Supplementary Fig. 11f) and lower metastasis-free survival (Supplementary Fig. 11g). These data highlight the correlation between higher fascin expression and metastasis and death in human breast caner patients.

METHODS SUMMARY

Affinity purification

4T1 tumor cells were lysed and the cell extract was then mixed with biotin-labeled macroketone or free biotin for 2 hours at 4°C with gentle rotation. Recombinant streptavidin-agarose beads (Pierce, IL) were added to the cell extract and the incubation was continued for another 2 hours with gentle rotation. The mixtures were then loaded onto the Poly-Prep chromatography column. After extensive wash with cell lysis buffer, samples were eluted by elution buffer. The elute was further concentrated by Centricon P-20 (Millipore, MA) and separated by SDS-PAGE. The gel was stained by Coomassie Blue and the indicated band was cut out for mass spectrometry and peptide sequencing analyses.

Breast Tumor Metastasis in Mice

All animal work was performed in compliance with the Institutional Animal Care and Use Committee of the Weill Medical College. Spontaneous 4T1 mouse breast tumor metastasis assay was done as described before [5,26]. In experimental lung metastasis experiments, NOD-SCID immunodeficient mice were used. MDA-MB-231 human breast tumor cells expressing the TGL reporter were trypsinized and washed with PBS. Subsequently 1×10^6 cells in 0.2 ml PBS were injected into the lateral tail vein. Luciferase-based, noninvasive bioluminescent imaging and analysis were performed with an IVIS Imaging System (Xenogen).

Crystallization and Structure Determination

To obtain crystals of the fascin-macroketone complex, the protein was incubated for one hour at room temperature in the protein buffer implemented with 2 mM macroketone. Crystallization was performed by the vapour diffusion hanging drop method at 20°C. Fascin crystallized in 100 mM Hepes, pH 8.0, 16% PEG4000, 1% isopropanol. Both crystals (fascin without or with macroketone) belong to C2 space group. X-ray diffraction data were recorded at National Synchrotron Light Source beamline X6A and X4C at Brookhaven National Laboratory. A partial structure was initially solved by the MR-SAD method using a seleni-methionine derivative sample that diffracted to 2.1 Å and a fraction of the 1DFC pdb file. This model was subsequently extended by iterative model building and refinement cycles using COOT and REFMAC5.

FULL METHODS

Materials

Mouse 4T1 mammary tumor cells and human MDA-MB-231 breast tumor cells were obtained from ATCC and have been described before [31,32]. 4T1 cells were cultured in RPMI 1640 medium supplemented with 10% FBS. MDA-MB-231 cells were cultured in DMEM supplemented with 10% FBS. Macroketone and biotin-conjugated macroketone were custom synthesized through outside companies.

Affinity purification

4T1 tumor cells were lysed in cell lysis buffer (50 mM Tris-HCl at pH 7.4, 150 mM NaCl, 1% NP40, 0.1% SDS, and protease inhibitors: 1 mM PMSF, 10 μg/ml leupeptin, pepstatin and aprotinin). The cell extract was then mixed with biotin-labeled macroketone or free biotin for 2 hours at 4°C with gentle rotation. Streptavidin beads (Pierce, IL) were added to the cell extract and the incubation was continued for another 2 hours with gentle rotation. The mixtures were then loaded onto the Poly-Prep chromatography column. After extensive wash with cell lysis buffer (with NaCl increased to 300 mM), samples were eluted by elution buffer (0.1 M glycine-HCl at pH 2.8) for 3 times. The elute was further concentrated by Centricon P-20 (Millipore, MA) and separated by SDS-PAGE. The gel was stained by Coomassie Blue and the indicated band was cut out for mass spectrometry and peptide sequencing analyses.

RNA interference

RNAi of fascin was performed in 4T1 mouse breast tumor and MDA-MB-231 human breast tumor cells using pSUPER vector (Oligoengine). The target sequences of the two pairs of mouse fascin were GGTGGGCAAAGATGAGCTC and GTGGAGCGTGCACATCGCC. The target sequences of the two pairs of human fascin were GGTGGGCAAGGACGAGCTC and GCCTGAAGAAGAAGCAGAT. Control shRNA was an shRNA that targets a LacZ sequence.

In Vitro Wound-healing Assay

Cell migration assays were performed as described previously [32,33]. Cells were allowed to form a confluent monolayer in a 24-well plate coated with gelatin before wounding. The wound was made by scraping a conventional pipette tip across the monolayer. The migration was induced by adding medium supplemented with 10% FBS. When the wound for the positive control closed, cells were fixed with 3.7% formaldehyde and stained with crystal violet staining solution.

Boyden Chamber Cell Migration Assay

Cells (5×10^4) suspended in starvation medium were added to the upper chamber of an insert (6.5 mm diameter, 8-μm pore size, Becton Dickenson), and the insert was placed in a 24-well dish containing starvation medium with or without 10% FBS [32,33]. When used, inhibitors were added to both chambers. Migration assays were carried out for 4~6 hours and cells were fixed with 3.7% formaldehyde. Cells were stained with crystal violet staining solution, and cells on the upper side of the insert were removed with a cotton swab. Three randomly selected fields (10 × objectives) on the lower side of the insert were photographed, and the migrated cells were counted. The migration was expressed as either the average number of migrated cells in a field or as percentage of migrated cells in positive control. Percentage was calculated with the formula $P=100 \times (M–M_{pc})/M_{pc}$, where P is the percentage of migrated cells, M is the number of migrated cells, M_{pc} is the number of migrated cells in negative controls, and M_{pc} is the number of migrated cells in positive controls.

Cell Invasion Assay

Cells (1×10^5) suspended in starvation medium were added to the upper chamber of a Matrigel-coated insert (6.5 mm diameter, 8-μm pore size, Becton Dickenson), and the insert was placed in a 24-well dish containing medium with or without serum. When used, inhibitors were added to both chambers. Invasion assays were carried out for 16 hours and cells were fixed with 3.7% formaldehyde. Cells were stained with crystal violet staining solution, and cells on the upper side of the insert were removed with a cotton swab. Three randomly selected fields (10 × objectives) on the lower side of the insert were photographed, and the cells on the lower surface of the insert were counted.

Protein Expression and Purification

Recombinant GST-fascin fusion protein was produced in BL21 *Escherichia coli*. A 1-liter culture wasgrown to an A_{600} reading of 1.0 and then induced by additionof 0.3 mM isopropyl 1-thio-D-galactopyranoside (IPTG) for 12 hours at 25°C. Cells were flash frozen and then lysed by sonication in Tris-buffered saline. The supernatant was then incubated with glutathione-Sepharose for 2 h at 4°C. After extensive washing, GST-fascin was eluted and concentrated with a Centricon Plus-20 (Millipore). To remove the GST tag from the fusion protein, beads were incubated with thrombin overnight at 4°C. The supernatant was collected and concentrated.

GST-fascin and Biotin-macroketone Interaction

Purified recombinant fascin protein or control protein were incubated with biotin-macroketone for 2 h at 4°C. Proteins associated with biotin-macroketone were precipitated with Ultralink-immobilized Strepavidin agarose (Pierce). After extensive washing, bound proteins were eluted with SDS sample buffer and resolved by 10% SDS-PAGE.

F-Actin Bundling Assay

Actin bundling activity was measured by low speed centrifugation assay and fluorescence microscopy. In low-speed centrifugationassay, monomeric rabbit G-actin was induced to polymerize at room temperature in F-actin buffer (20 mM Tris–HCl at pH 8, 1 mM ATP, 1 mM DTT, 2 mM $MgCl_2$ and 100 mM KCl). Recombinant fascin proteins or control buffer were subsequently incubated with F-actin for 60 min at room temperature and centrifuged for 30 min at 10,000g in an Eppendorf 5415D table-top centrifuge. Both supernatants and pellets were dissolved in an equivalent volume of SDS sample buffer, and the amount of actin was determined by SDS-PAGE. We measured the intensities of fascin proteins in Coomassie-stained gels and then calculated the “relative actin bundling activity” by the following formula. $P=100 \times M_p/M_{pc}$, where P is the relative actin bundling activity, M_p is the percentage of actin that is present in pellet when mixed with different concentrations of fascin protein. It alone can be calculated by intensity in pellet/(intensity in pellet + intensity in supernatant). M_{pc} is the percentage of actin that is present in pellet when mixed with 0.25 μM fascin, which is used at a saturated concentration determined in our control experiment.

In fluorescence microscopy, monomeric G-actin was polymerized as described above. F-actin was mixed with recombinant fascin protein in F-buffer and incubated at room temperature for 30 min. Actin was then labeled by adding 5 % rhodamine–phalloidin to the mixture. The samples were mounted between a slide and a coverslip coated with poly-lysine and imaged by fluorescence microscopy. Three randomly selected fields (10 × objectives) were photographed, and the bundles were counted. The Bundles/Field was expressed as the average number of bundles ± S.D.

Immunofluorescence Microscopy

Cells cultured on gelatin-coated glass coverslips were fixed with 3.7% formaldehyde in PBS for 10 min at room temperature, permeabilized with 0.1% Triton X-100 for 5 min, and then washed with PBS three times. To block nonspecific binding, the cells were incubated with a solution of PBS containing 1% bovine serum albumin for 30 min and then incubated with primary antibody at appropriate dilutions for 1 h. After incubation with primary antibody, cells were washed three times with PBS and incubated with fluorescence-conjugated secondary antibody (Molecular Probes). The coverslips were then fixed onto slides and imaged using a Zeiss fluorescence microscope.

Electron Microscopy

Samples were absorbed onto freshly glow-discharged, carbon-coated copper grids for 2 minutes and stained with 2% uranyl acetate. Grids were examined using a Zeiss electron microscopy at an accelerating voltage of 80 kV.

4T1 Breast Tumor Metastasis in Mice

All animal work was performed in compliance with the Institutional Animal Care and Use Committee of the Weill Medical College. Spontaneous 4T1 mouse breast tumor metastasis assay was done as described before [31,34]. Female BALB/c mice (6–8 week old) were purchased from the Jackson Laboratory. 4T1 tumor cells (1×10^5) were injected subcutaneously into the abdominal mammary gland area of mice using 0.1 ml of a single-cell suspension in PBS on Day 0. The dosage of tumor implantation was empirically determined to give rise to tumors of about 10 mm in diameter in untreated wild type mice within 21–23 days. Starting on Day 7, when the tumors averaged about 4–5 mm in diameter, test compounds or control PBS saline were given every day by intraperitoneal injection at 10 mg/kg per mouse until Day 25. On Day 28, the mice were sacrificed. This dosage regiment was well tolerated with no signs of overt toxicity. Every group included 5 mice. Primary tumors were measured using electronic calipers on the day the mice were sacrificed. Numbers of metastatic 4T1 cells in lungs were determined by the clonogenic assay. In brief, lungs were removed from each mouse on Day 28, finely minced and digested in 5 ml of enzyme cocktail containing 1 × PBS and 1 mg/ml collagenase type IV for 2 hours at 37°C on a platform rocker. After incubation, samples were filtered through 70 μm nylon cell strainers and washed twice with PBS. Resulting cells were suspended, plated with a series of dilutions in 10 cm tissue culture dishes in RPMI1640 medium containing 60 μM thioguanine for clonogenic growth. Since 4T1 tumor cells are resistant to 6-thioguanine, metastasized tumor cells formed foci after 14 days, at which time they were fixed with methanol and stained with 0.03% methylene blue for counting.

MDA-MB-231 Human Breast Tumor Lung Colonization in Mice

NOD-SCID immunodeficient mice were used for experimental lung colonization experiments. MDA-MB-231 human breast tumor cells expressing the TGL reporter were trypsinized and washed with PBS. This artificial TGL reporter gene encodes a triple fusion protein with herpes simplex virus 1 thymidine kinase fused to the N-terminus of enhanced GFP and firefly luciferase fused to the C-terminus of GFP [34,35]. Subsequently 1×10^6 cells in 0.2 ml PBS were injected into the lateral tail vein. Luciferase-based, noninvasive bioluminescent imaging and analysis were performed with an IVIS Imaging System (Xenogen).

Microarray Gene Expression Analysis

Gene expression data for fascin was extracted from each tumor sample and mean-centered across all samples for each. Tissues from primary breast cancers were obtained from therapeutic procedures performed as part of routine clinical management at Memorial Sloan-Kettering Cancer Center. All research procedures using human tissue were approved by the MSKCC institutional review board [36]. Tissues were snap-frozen in liquid nitrogen and stored at −80°C. Each sample was examined histologically using hemotoxylin- and eosin-stained cryostat sections. Regions were manually dissected from the frozen block to provide a consistent tumor cell content of more than 70% in tissues used for analysis. Total RNA was extracted from frozen tissue by homogenization in guanidinium isothiocyanate-based buffer (Trizol; Invitrogen, Carlsbad, CA), purified using RNAeasy (Qiagen, Valencia, CA)

and examined for quality using denaturing agarose gel. Complementary DNA was synthesized from RNA using a T7-promoter-tagged oligo-dT primer. RNA target was synthesized from cDNA by in vitro transcription, and labeled with biotinylated nucleotides (Enzo Biochem, Farmingdale, NY). Gene expression analysis was performed using HG-U133A and U133B oligonucleotide microarrays according to the manufacturer's instructions (Affymetrix, Santa Clara, CA). To identify the differential gene expression, we used two different measures: fold change (ratio) between the normalized means of each group of samples and a Student's t-test. The microarray data had been previously deposited at Gene Expression Omnibus (GEO) under accession number GSE2603.

Human fascin-1 expression and purification

The recombinant human fascin-1 was expressed as GST-fusion protein in *E. coli.* Typically, a 1 liter 2YT medium with antibiotic was inoculated with 3ml overnight BL21/DE3 culture transformed with pGEX4T-Fascin1 plasmid and grown at 37°C until OD_{600} reached ~0.8. The culture was then transferred to 22 °C and 0.1 mM IPTG was added for induction. After overnight induction, the bacteria were harvested by centrifugation at 5,000 rpm for 10 min. The bacteria pellet was snap frozen with liquid nitrogen and suspended in 30 ml 1× PBS supplemented with 0.2 mM PMSF, 1 mM DTT, 1% Triton X-100 and 1 mM EDTA. After sonication, the suspension was centrifuged at 15,000 rpm for 60 min to remove the cell debris. The supernatant was then incubated with 4 ml glutathione beads (Sigma) at 4 °C for 2 hours. After extensive wash with PBS, the beads were resuspended in 10 ml thrombin cleavage buffer (20 mM Tris, pH 8.0, 150 mM NaCl, 2 mM $CaCl_2$, 1 mM DTT). Human Fascin-1 was released from the beads by incubating with 40–100 unit of thrombin overnight at 4°C. After centrifugation, 0.2 mM PMSF was added to supernatant to inactivate the remnant thrombin activity. The fascin protein was further purified with a Superdex 200 gel filtration column and concentrated with Centricon to about 80mg/ml. The typical yield from a 1 liter culture is about 40 mg.

Crystallization and structure determination

The concentrated protein stock solution was diluted with the protein buffer (20 mM Tris, pH 8.0, 40 mM KBr, 0.5 mM EDTA, 1 mM DTT) to 15 mg/ml prior crystallization. In order to obtain crystals of the fascin-macroketone complex, the protein was incubated for one hour at room temperature in the protein buffer implemented with 2 mM macroketone. Crystallization was performed by the vapour diffusion hanging drop method at 20°C. Fascin crystallized in 100 mM Hepes, pH 8.0, 16% PEG4000, 1% isopropanol. Both crystals (fascin without or with macroketone) belong to C2 space group. Crystals were briefly transferred to the cryo-solution which consisted of the crystallization solution implemented with 15% glycerol and flash-cooled in liquid nitrogen. X-ray diffraction data were recorded at National Synchrotron Light Source beamline X6A and X4C at Brookhaven National Laboratory. A partial structure was initially solved by the MR-SAD method using a seleni-methionine derivative sample that diffracted to 2.1 Å and a fraction of the 1DFC pdb file. This model was subsequently extended by iterative model building and refinement cycles using COOT [37] and REFMAC5 [38]. The fascin structure was solved by the molecular replacement method using the Se-Met MR-SAD structure as starting model and finally refined following the same procedure. The diffraction of some fascin crystals was

dramatically improved by an “annealing” process involving one freeze-thaw-freeze treatment. A 1.8 Å dataset obtained from an annealed crystal rendered dramatically improved electronic density map, which was unambiguous throughout almost the entirety of both molecules in the asymmetric unit. The asymmetric unit contains 2 mostly complete molecules with the exception of 4 highly flexible loops (residues 1–7, 49–54, and 245–247 in chain A and residues 1–7 and 300–303 in chain B) with poorly defined electron density. For the crystals of the complex of fascin and macroketone, one of the two molecules in the asymmetric unit is relatively disordered. An approximately 4σ peak was observed in the difference density map (Supplementary Fig. 7), near the surface of beta-trefoil 4 of molecule A, on the side facing the cleft between trefoil 4 and trefoil 1. The ring structure was easily discernable in the difference map, while densities for the side chains were missing. The approximate orientation of the macroketone molecule was derived by fitting the macrolide ring into the density while having the possible polar interactions between macroketone and fascin in mind.

Statistical Analysis

Data are expressed as mean ± S.D. and analyzed by Student’s *t* test with significance defined as $p < 0.05$.

Supplementary Material

Refer to Web version on PubMed Central for supplementary material.

Acknowledgments

JJZ and XYH dedicate this paper to the memory of Yonghong Zhang, who died of cancer September 12, 2009. We are very grateful to Dr. William Gerald (deceased) at MSKCC for letting us examine his DNA microarray data on human breast tumor samples for the fascin expression. We thank Dr. S. Almo for the fascin plasmid, Dr. S. Danishefsky and colleagues for the biotin-conjugated macroketone used in the initial exploration of the conditions for protein purification, and members in the J. Massague lab for teaching the use of the IVIS Imaging system. We are grateful to Dr. S. Almo and his colleagues, Drs. H. Wu and J. Wu for help with the crystallization experiments. We also appreciate the beamtime and the assistance of the personnel at the beamlines X6A and X4C of the National Synchrotron Light Source. We are grateful to Drs. D. Eliezer, T. Maack, L. Palmer, H. Wu, and members of our laboratory for critically reading the manuscript. This work was supported by grants from NIH (CA136837) and the Department of Defense (W81XWH-06-1-0362).

References

1. Nakae K, et al. Migrastatin, a novel 14-membered lactone from Streptomyces sp. MK929–43F1. J Antibiot (Tokyo). 2000; 53:1228–30. [PubMed: 11132973]
2. Woo EJ, et al. Migrastatin and a new compound, isomigrastatin, from Streptomyces platensis. J Antibiot (Tokyo). 2002; 55:141–6. [PubMed: 12002995]
3. Njardarson JT, Gaul C, Shan D, Huang XY, Danishefsky SJ. Discovery of potent cell migration inhibitors through total synthesis: lessons from structure-activity studies of (+)-migrastatin. J Am Chem Soc. 2004; 126:1038–40. [PubMed: 14746469]
4. Gaul C, et al. The migrastatin family: discovery of potent cell migration inhibitors by chemical synthesis. J Am Chem Soc. 2004; 126:11326–37. [PubMed: 15355116]
5. Shan D, et al. Synthetic analogues of migrastatin that inhibit mammary tumor metastasis in mice. Proc Natl Acad Sci U S A. 2005; 102:3772–6. [PubMed: 15728385]

6. Ju J, et al. Evaluation of new migrastatin and dorrigocin congeners unveils cell migration inhibitors with dramatically improved potency. Bioorg Med Chem Lett. 2008; 18:5951–4. [PubMed: 18684620]
7. Otto JJ, Kane RE, Bryan J. Formation of filopodia in coelomocytes: localization of fascin, a 58,000 dalton actin cross-linking protein. Cell. 1979; 17:285–93. [PubMed: 378407]
8. Bryan J, Kane RE. Separation and interaction of the major components of sea urchin actin gel. J Mol Biol. 1978; 125:207–24. [PubMed: 731692]
9. Yamashiro-Matsumura S, Matsumura F. Purification and characterization of an F-actin-bundling 55-kilodalton protein from HeLa cells. J Biol Chem. 1985; 260:5087–97. [PubMed: 3886649]
10. Vignjevic D, et al. Formation of filopodia-like bundles in vitro from a dendritic network. J Cell Biol. 2003; 160:951–62. [PubMed: 12642617]
11. Vignjevic D, et al. Role of fascin in filopodial protrusion. J Cell Biol. 2006; 174:863–75. [PubMed: 16966425]
12. Adams JC. Roles of fascin in cell adhesion and motility. Curr Opin Cell Biol. 2004; 16:590–6. [PubMed: 15363811]
13. Maitra A, et al. Immunohistochemical validation of a novel epithelial and a novel stromal marker of pancreatic ductal adenocarcinoma identified by global expression microarrays: sea urchin fascin homolog and heat shock protein 47. Am J Clin Pathol. 2002; 118:52–9. [PubMed: 12109856]
14. Pelosi G, et al. Independent value of fascin immunoreactivity for predicting lymph node metastases in typical and atypical pulmonary carcinoids. Lung Cancer. 2003; 42:203–13. [PubMed: 14568688]
15. Hashimoto Y, Shimada Y, Kawamura J, Yamasaki S, Imamura M. The prognostic relevance of fascin expression in human gastric carcinoma. Oncology. 2004; 67:262–70. [PubMed: 15557788]
16. Hashimoto Y, Skacel M, Adams JC. Roles of fascin in human carcinoma motility and signaling: prospects for a novel biomarker? Int J Biochem Cell Biol. 2005; 37:1787–804. [PubMed: 16002322]
17. Yoder BJ, et al. The expression of fascin, an actin-bundling motility protein, correlates with hormone receptor-negative breast cancer and a more aggressive clinical course. Clin Cancer Res. 2005; 11:186–92. [PubMed: 15671545]
18. Zigeuner R, Droschl N, Tauber V, Rehak P, Langner C. Biologic significance of fascin expression in clear cell renal cell carcinoma: systematic analysis of primary and metastatic tumor tissues using a tissue microarray technique. Urology. 2006; 68:518–22. [PubMed: 16979727]
19. Rodriguez-Pinilla SM, et al. Prognostic significance of basal-like phenotype and fascin expression in node-negative invasive breast carcinomas. Clin Cancer Res. 2006; 12:1533–9. [PubMed: 16533778]
20. Minn AJ, et al. Genes that mediate breast cancer metastasis to lung. Nature. 2005; 436:518–24. [PubMed: 16049480]
21. Wu JM, et al. Heterogeneity of breast cancer metastases: comparison of therapeutic target expression and promoter methylation between primary tumors and their multifocal metastases. Clin Cancer Res. 2008; 14:1938–46. [PubMed: 18381931]
22. Ono S, et al. Identification of an actin binding region and a protein kinase C phosphorylation site on human fascin. J Biol Chem. 1997; 272:2527–33. [PubMed: 8999969]
23. Mosialos G, et al. Epstein-Barr virus infection induces expression in B lymphocytes of a novel gene encoding an evolutionarily conserved 55-kilodalton actin-bundling protein. J Virol. 1994; 68:7320–8. [PubMed: 7933116]
24. Cant K, Cooley L. Single amino acid mutations in Drosophila fascin disrupt actin bundling function in vivo. Genetics. 1996; 143:249–58. [PubMed: 8722779]
25. Minn AJ, et al. Distinct organ-specific metastatic potential of individual breast cancer cells and primary tumors. J Clin Invest. 2005; 115:44–55. [PubMed: 15630443]
26. Yang S, Zhang JJ, Huang XY. Orai1 and STIM1 are critical for breast tumor cell migration and metastasis. Cancer Cell. 2009; 15:124–34. [PubMed: 19185847]
27. Grothey A, Hashizume R, Sahin AA, McCrea PD. Fascin, an actin-bundling protein associated with cell motility, is upregulated in hormone receptor negative breast cancer. Br J Cancer. 2000; 83:870–3. [PubMed: 10970687]

28. Hashimoto Y, Parsons M, Adams JC. Dual actin-bundling and protein kinase C-binding activities of fascin regulate carcinoma cell migration downstream of Rac and contribute to metastasis. Mol Biol Cell. 2007; 18:4591–602. [PubMed: 17855511]
29. Vignjevic D, et al. Fascin, a novel target of beta-catenin-TCF signaling, is expressed at the invasive front of human colon cancer. Cancer Res. 2007; 67:6844–53. [PubMed: 17638895]
30. van't Veer LJ, et al. Gene expression profiling predicts clinical outcome of breast cancer. Nature. 2002; 415:530–6. [PubMed: 11823860]
31. Shan D, et al. Synthetic analogues of migrastatin that inhibit mammary tumor metastasis in mice. Proc Natl Acad Sci U S A. 2005; 102:3772–6. [PubMed: 15728385]
32. Yang S, Huang XY. Ca2+ Influx through L-type Ca2+ Channels Controls the Trailing Tail Contraction in Growth Factor-induced Fibroblast Cell Migration. J Biol Chem. 2005; 280:27130–7. [PubMed: 15911622]
33. Shan D, et al. The g protein galpha(13) is required for growth factor-induced cell migration. Dev Cell. 2006; 10:707–18. [PubMed: 16740474]
34. Yang S, Zhang JJ, Huang XY. Orai1 and STIM1 are critical for breast tumor cell migration and metastasis. Cancer Cell. 2009; 15:124–34. [PubMed: 19185847]
35. Ponomarev V, et al. A novel triple-modality reporter gene for whole-body fluorescent, bioluminescent, and nuclear noninvasive imaging. Eur J Nucl Med Mol Imaging. 2004; 31:740–51. [PubMed: 15014901]
36. Doane AS, et al. An estrogen receptor-negative breast cancer subset characterized by a hormonally regulated transcriptional program and response to androgen. Oncogene. 2006; 25:3994–4008. [PubMed: 16491124]
37. Emsley P, Cowtan K. Coot: model-building tools for molecular graphics. Acta Crystallogr D Biol Crystallogr. 2004; 60:2126–32. [PubMed: 15572765]
38. Vagin AA, et al. REFMAC5 dictionary: organization of prior chemical knowledge and guidelines for its use. Acta Crystallogr D Biol Crystallogr. 2004; 60:2184–95. [PubMed: 15572771]

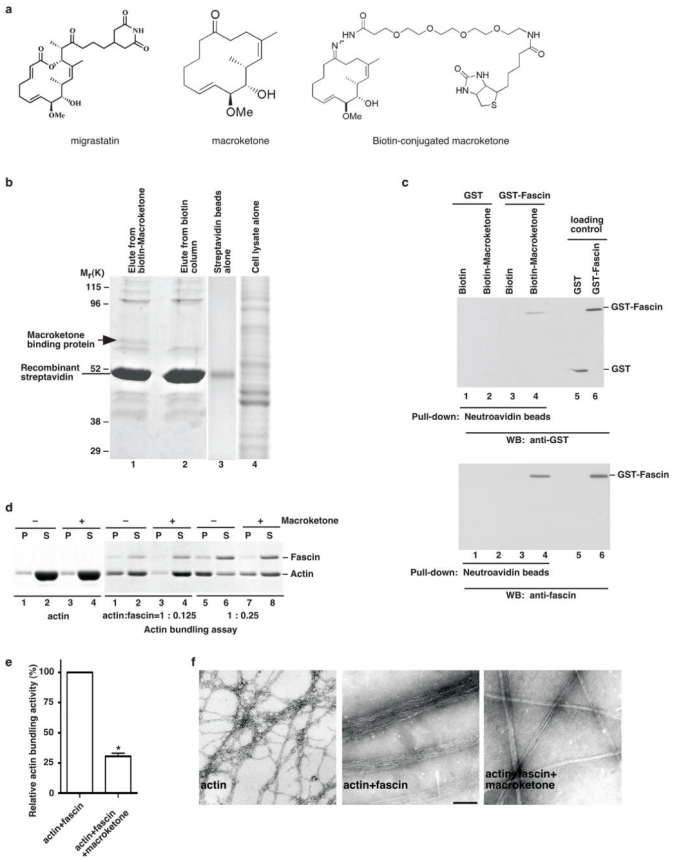

Figure 1.

Identification of fascin as a macroketone target. **a,** Diagram of the structures of migrastatin, one of its analogue (the macroketone core), and the biotin-conjugated macroketone core. **b,** Coomassie blue stain of the SDS/PAGE gel after protein affinity purification. The arrow indicated the band identified as mouse fascin 1. **c,** Direct interaction of fascin with macroketone. Agarose beads with biotin-conjugated macroketone (10 μM) or biotin (10 μM) were mixed with GST-fascin or GST. Data are representative of three experiments with similar results. **d,** Assay of the actin-bundling activity by the low-speed co-sedimentation assay. Polymerized F-actin (1 μM) was incubated with 0.125 μM or 0.25 μM purified fascin in the presence or absence of macroketone (10 μM). Supernatants (S) or pellets (P) were analyzed by SDS-PAGE followed by Coomassie blue staining. A representative of five experiments with similar outcomes was shown. **e,** Quantification of F-actin bundling assays from **d**. Results are mean ± SD (n=5, *, $p<0.05$). **f,** Electron microscopy of fascin-induced F-actin bundles in the presence or absence of macroketone. F-actin (1 μM) was incubated with fascin (0.125 μM) in the presence or absence of macroketone (10 μM). Representative images were shown. Scale bar: The scale bar represents 50 nm. Results are mean ± SD (n=7, *, $p<0.05$).

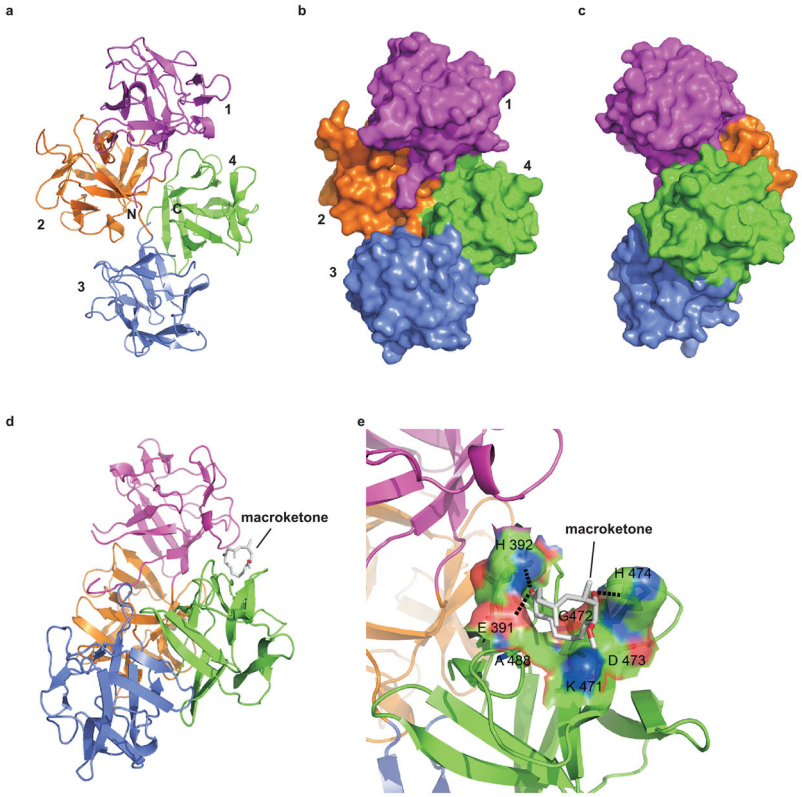

Figure 2.

X-ray crystal structures of fascin and of the complex of fascin and macroketone. **a,** Structure of fascin shown as ribbon diagram, viewed from the N- and C-terminal plane. The four β-trefoil domains are colored magenta (Trefoil 1), orange (Trefoil 2), blue (Trefoil 3) and green (Trefoil 4). **b,** Surface presentation of fascin structure viewed in **a. c,** View of fascin turned clockwise 90° along the y-axis relative to the view in (**b). d,** Overall structure of the complex of fascin and macroketone. The macroketone molecule is shown as white stick model. **e,** Macroketone binding site. Residues involved in interactions with macroketone are shown as surface and hydrogen bonds are shown as dash lines.

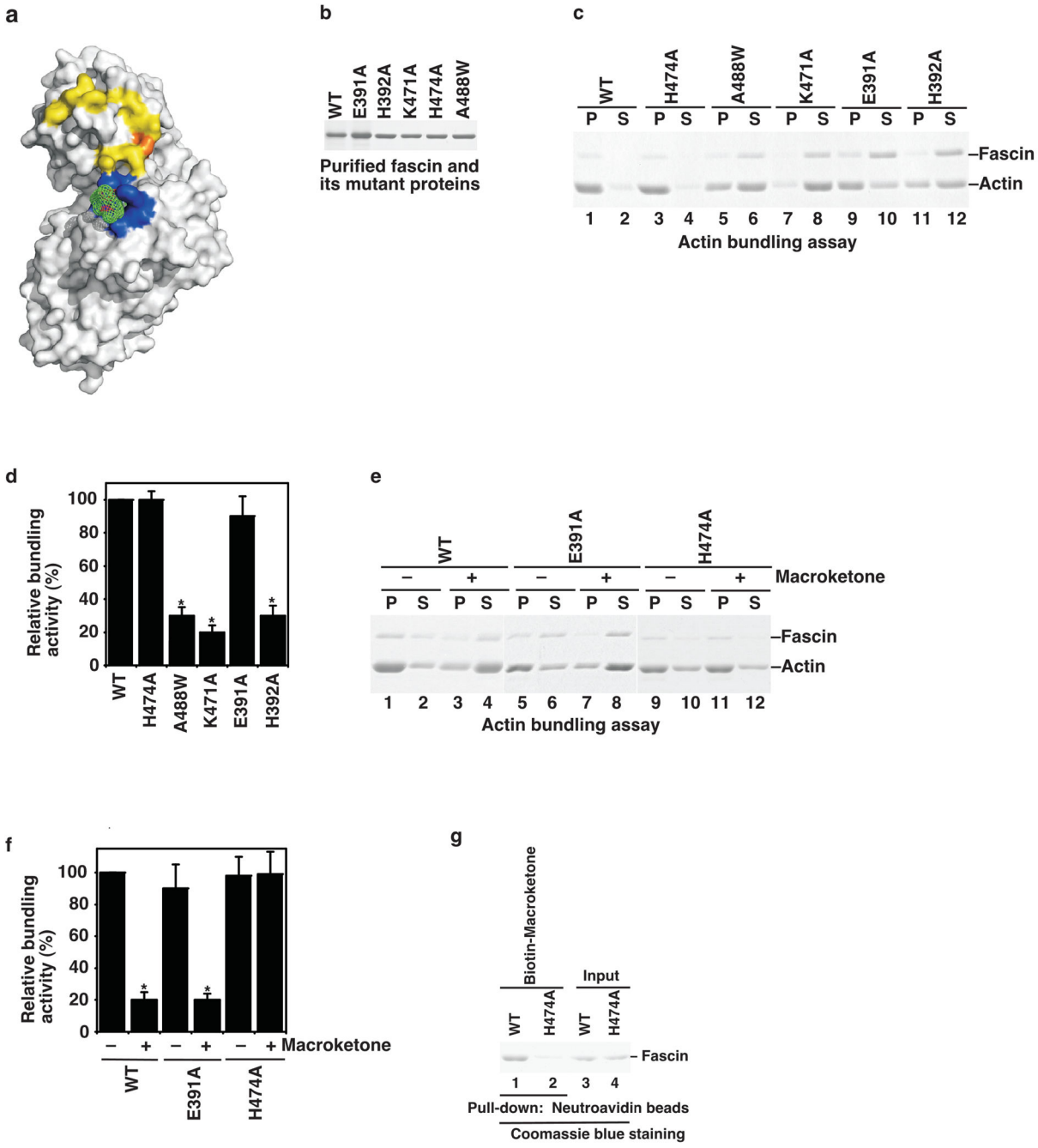

Figure 3.

Macroketone binding site overlaps with one of the actin-binding sites. **a,** Surface presentation of the structure of the complex of fascin and macroketone. Residues involved in macroketone binding are shown in blue. Sequences (residues 29–42) homologous to the MARCKS actin-binding site are colored yellow and PKC phosphorylation site (Ser39) is colored orange. Macroketone is shown as green mesh. **b,** Coomassie blue stain of purified fascin and its mutant proteins. **c, d,** Actin bundling assay for the wild-type fascin and its mutants. **e, f,** Sensitivity to macroketone. Wild-type fascin, E391A and H474A mutants of

fascin were assayed for their actin bundling activity in the absence or presence of macroketone (10 μM). Results are mean ± SD (n=3, $p<0.05$). **g**, H474A fascin mutant protein failed to bind biotin-macroketone. The residual H474A protein pulled down by biotin-macroketone (lane 2) was due to aggregates bound to the beads.

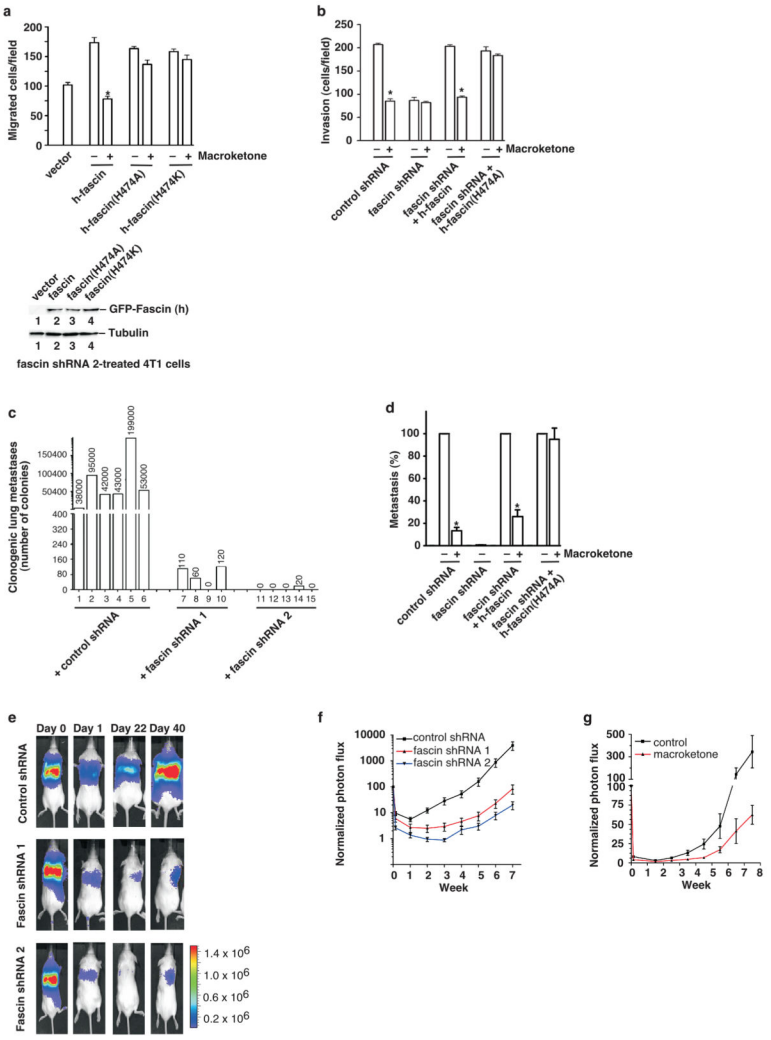

Figure 4.

Fascin His474 mutation renders tumor cell migration, invasion and metastasis resistant to macroketone. **a,** Boyden chamber cell migration assay of mouse fascin shRNA 2-treated 4T1 cells transfected with various mutants of GFP-human fascin (h-fascin) in the presence or absence of macroketone (10 μM). Bottom panel shows the over-expression of various fascin mutants in mouse fascin shRNA 2-treated 4T1 cells. Results are mean ± SD (n=5, $p<0.05$). **b,** In vitro Matrigel invasion assay with mouse fascin shRNA-treated 4T1 cells overexpressing wild-type human fascin or fascin(H474A) mutant in the presence or absence of macroketone (10 μM). Results are mean ± SD (n=5, $p<0.05$). **c,** Total number of metastatic colonies in lungs of individual mice four weeks after injecting 4T1 cells expressing control shRNA and two fascin shRNAs. 1 to 15 (x-axis) are mouse identification numbers. **d,** Tumor metastasis assay with mouse fascin shRNA-treated 4T1 cells overexpressing wild-type human fascin or fascin(H474A) mutant in the presence or absence of macroketone (10 mg/kg). Fascin shRNA group was compared with control shRNA group. Results are mean ± SD (n=5~6, $p<0.05$). **e,** Representative noninvasive bioluminescence images of mice at the indicated dates after injecting human MDA-MB-231 cells expressing

control shRNA and two fascin shRNAs. **f,** Normalized photon flux of noninvasive bioluminescence images of mice at the indicated dates after injecting human MDA-MB-231 cells expressing control shRNA and two fascin shRNAs. Results are mean ± SD. **g,** Normalized photon flux of noninvasive bioluminescence images of mice at the indicated dates after injecting human MDA-MB-231 cells in the presence or absence of macroketone (10 mg/kg). Results are mean ± SD.